ACS APPLIED MATERIALS & INTERFACES

Research Article

www.acsami.org

Adsorption Behavior of EDTA-Graphene Oxide for Pb (II) Removal

Clemonne J. Madadrang,[†] Hyun Yun Kim,[†] Guihua Gao,[‡] Ning Wang,[‡] Jun Zhu,[‡] Huan Feng,[§] Matthew Gorring,[§] Marc L. Kasner,[†] and Shifeng Hou*,[†]

[†]Department of Chemistry & Biochemistry and [§]Department of Earth and Environment Studies, Montclair State University, Montclair New Jersey 07043, United States

[‡]Department of Chemistry, Jining Medical College, Jining, Shandong Province 272113, P.R. China

ABSTRACT: Chelating groups are successfully linked to graphene oxide (GO) surfaces through a silanization reaction between N-(trimethoxysilylpropyl) ethylenediamine triacetic acid (EDTA-silane) and hydroxyl groups on GO surface. EDTA-GO was found to be an ideal adsorbent for Pb(II) removal with a higher adsorption capacity. EDTA-modification enhances the adsorption capacity of GO because of the chelating ability of ethylene diamine triacetic acid. This study investigates the adsorption and desorption behaviors of heavy metal cations and the effects of solution conditions such as pH on Pb(II) removal. The adsorption capacity for Pb(II) removal was found to be 479 ± 46) mg/g at pH 6.8, and the adsorption process was completed within 20 min. The Langmuir adsorption model agrees well with the experimental data. The experimental results suggest that EDTA-GO can be reused after washed with HCl, suggesting potential applications in the environmental cleanup.

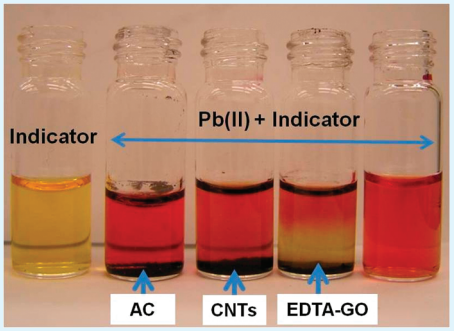

KEYWORDS: *graphene oxide, adsorbents, lead, EDTA*

1. INTRODUCTION

Water pollution due to the indiscriminate disposal of metal ions and organic contaminants has been a rising worldwide environmental concern. For example, wastewater from many industries such as metallurgical and chemical manufacturing, mining, battery, etc., contains one or more toxic metal ions.[1,2] For environmental protection, it is necessary to remove these metal contaminants from the wastewater before releasing into the environment.[3] Entire removal of heavy metals and organic contaminants in natural water resources can not only protect the environment itself, but also stop the toxic contaminant transfer in food chains. Traditional techniques for treatment of metal ions include reduction, coprecipitation, membrane filtration, ion exchange and adsorption. Among the above methods, the most promising process for the removal of metal ions is adsorption. Several adsorbents that have been studied for metal removal include activated carbon (AC),[4] zeolite,[5] inorganic materials,[6,7] and resins. However, these adsorbents have been suffering from either low adsorption capacities or low efficiencies. Therefore, tremendous effort has been made in recent years to seek new adsorbents and develop new techniques. An ideal adsorbent should have the ability to rapidly and efficiently remove toxic contaminants from environments to a safety level. Nanotechnology and nanomaterials have gradually demonstrated playing an important role in this aspect.[8−11] The benefits from the use of nanomaterials for metal removal may derive from their enhanced reactivity, higher specific surface area and sequestration characteristics. So far, a variety of nanomaterials are in various stages of research and development, each possessing unique functionalities that are potentially applicable to the remediation of industrial effluents, groundwater, surface water, and drinking water. Carbon-based nanomaterials are one type of these materials that have potential applications in the wastewater treatment system.[11,12]

Carbon-based nanomaterials have been studied as superior adsorbents for their potential environmental applications to remove pollutants, such as organic pollutants and metals with high capacity and selectivity in aqueous solutions.[11,13−19] One of the advantages of carbon-based nanoparticles as attractive adsorbents is that they have much larger specific surface areas.[20] For example, carbon nanotubes (CNTs) have been suggested as "a superior adsorbent" for dioxins with excellent adsorption capacity because CNTs provide geometry sites for stronger interactions with organic pollutants. Many methods have been exploited for the preparation of various functional CNTs. The surface oxidized CNTs have showed exceptional adsorption capacity and high adsorption efficiency for metal removal.[20−26] Earlier studies indicate that CNTs can be promising adsorption materials used for environmental protection regardless of their high cost at present. The prospect of using carbon nanotubes for water pollution control appears to be very favorable, but large-scale applications of CNTs in the near future are limited by cost and availability. So far, it is difficult to predict in general which of these CNTs-based adsorbents will be commercialized because of cost concerns. Therefore, the rational design of

Received: May 18, 2011
Accepted: February 3, 2012
Published: February 3, 2012

adsorbents with lower cost is a challenge. Greater efforts are made to seek the lower cost carbon-based nanomaterials as adsorbents for environmental applications. Graphene or graphene oxide, a CNT-substituted material and a product of graphite from an oxidization process, may be an ideal material for wastewater treatment. Normally, graphene obtained from graphite exists in two states, i.e., graphene oxide (GO) and reduced graphene oxide (RGO).[27−29] Graphene oxide (GO) is water-soluble with low conductivity while RGO has good conductivity with poor solubility in water.[30] The oxidation process of graphite to graphene oxide can introduce abundant functional groups on GO surface that can be used as anchoring sites for metal ion complexation, making it a potential material as a super adsorbent.[31] Unlike CNTs, which need a special oxidation process to introduce hydrophilic groups for metal removal, the formation process from graphite to GO already introduces many functional groups, such as −COOH, −C═O and −OH on GO surface. These groups are the essential chemical skeletons for an ideal adsorbent.[31−38]

Ethylenediaminetetraacetic acid (EDTA) is well-known for forming stable chelates with metal ions. Therefore, it can be ideally used for metal removal.[39,40] Immobilization of EDTA on different supporting materials for adsorption purpose as received widespread attention, these substrate include silica gel,[41] polymer resin,[42−44] and cellulose.[40,45,46] In a previous study, we reported a method to chemically functionalize graphene sheets with N-(trimethoxysilylpropyl) ethylenediamine triacetic acid via a silanization reaction.[47−49] EDTA-GO is found to be an ideal adsorbent for heavy metal removal. Upon linked to substrate, EDTA serves as a chelating group to form a stable chelate with metal ions. This laboratory research was designed to investigate the adsorption behavior of Pb(II) on EDTA-GO surface and the potential applications of EDTA-GO for heavy metal removal. We found that Pb(II) concentration in Pb(II) contaminated water could be decreased to ∼0.5 ppb or less after the treatment with EDTA-GO.

2. EXPERIMENTAL SECTION

2.1. Materials. Graphite, activated carbon powders, standard Pb(II) solution (1.000 mg/mL Pb (II) in 2% HNO_3), sulfuric acid, HCl, and other chemical reagents used in our experiment are commercial products purchased from Aldrich. These reagents and solvents were used without further purification. Pb(II) metal solutions in various pH conditions were prepared by directly diluting 1.000 mg/mL Pb(II) solution with the buffer solutions prepared from NaAc-HAc and NH_4Cl-NH_3.

Graphene oxide was prepared by oxidizing natural graphite with strong oxidants such as H_2SO_4 and $KMnO_4$ using a modification of Hummers and Offeman's method in our laboratory.[48,50] The sizes of single-layer graphene sheets vary from several hundred nanometers to several micrometers, depending on the initial graphite sizes.[48] Briefly, graphite powders were first preoxidized by sulfuric acid, $K_2S_2O_8$, and P_2O_5. Next, the preoxidized graphite was oxidized by concentrated H_2SO_4, $KMnO_4$, and 30% H_2O_2, and the products were filtered and washed with 0.1 M HCl and DI water. The resulting GO solid was dried in room temperature. EDTA-GO was finally obtained by reacting N-(trimethoxysilylpropyl) ethylenediamine triacetic acid (EDTA-silane) with GO in ethanol solution in a silylation process following by filtration and washing with methanol and water sequentially.[48] In this experiment, the mass percent of Si of EDTA-GO is determined to be 5.5 ± 1.2 wt %. To reduce graphene oxide (GO) to reduced graphene oxide (RGO), we thermally treated 0.1 g of EDTA-GO directly in an oven at 300 °C for 30 min under nitrogen protection. Upon reduction, the EDTA-GO changed color from brown to black (EDTA-RGO).

2.2. Equipment. The concentration of metal ions in a solution was analyzed using Perkin-Elmer 3110 Atomic Absorption Spectrometry (AAS), a Thermo Scientific ICAP 6000 Series ICP system, and a Thermal Fisher Evolution 300 UV−vis spectrum instrument. The Energy-dispersive X-ray spectroscopy (EDXS) was taken on a JEOL 2010F microscope (JEOL Ltd., Japan) with an energy dispersion X-ray (EDXS) analyzer. A Zeta-sizer Nano-ZS (Malvern, UK) was used for zeta potential measurement. The sample separation was achieved using a Thermo Scientific Sorvall centrifuge. Brunauer−Emmett−Teller (BET) surface area measurements were completed using a GAPP V-Sorb 4800S.

2.3. Characteristics of EDTA-GO. The zeta potential of EDTA-GO, GO and AC were measured using a Zeta-sizer Nano-ZS (Malvern, UK). Before the experiment, 10.0 mg of EDTA-GO, GO and AC were suspended in a 20.0 mL buffer solution with various pH values of 3.0, 4.5, 5.8, 6.8, 7.9, and 11.8, respectively. The suspensions were first sonicated for 30 min and then keep stirring overnight before the experiment. The pH values of the suspensions were measured before and after the experiment.

The total acidic and basic sites as functional groups on GO and EDTA-GO were determined following Boehm titration procedure.[51−54] To prepare a sample for Boehm titration, 0.1000 g of AC, GO, EDTA-GO, and EDTA-RGO was dispersed into 10.0 mL of DI water, and then 10.0 mL of 0.10 M NaOH and HCl solutions were added to the above solutions, respectively, sealed and stirred for 36 h. The suspensions were then filtrated and all the filtrated solutions were transferred into beakers and the solutions were titrated with 0.10 M standard HCl or NaOH solution.

2.4. Adsorption Experiments. To perform an adsorption isotherm analysis, a typical adsorption experiment was carried out by adding 10 or 25 mg of EDTA-GO to a 100 or 200 mL Pb(II) solution (in a plastic vial) at room temperature (25 ± 2 °C). The initial Pb concentrations varied from 5 ppm to 300 ppm (or mg/L), and the pH value of all Pb(II) solutions was maintained at 6.8 with a buffer solution. After adding EDTA-GO, the vial with solution was sealed and left for 24 h for enough reaction time to achieve the adsorption equilibrium state. Then, the mixture was filtered through a 0.2 μm pore size membrane. The Pb(II) concentration on the filtrate was carefully analyzed using AAS, ICP and UV spectrometry, which is identified as the equilibrium concentration of Pb(II) (C_e). The amount of Pb(II) adsorbed by the EDTA-GO was taken as the difference between the initial and equilibrium concentrations of Pb(II) in the solutions and the adsorption capacity (q_e, mg/g) of the Pb(II) adsorbed onto EDTA-GO was obtained from the following equation and used for further adsorption isotherm analysis:

$$q_e = \frac{(C_i - C_e)V}{w} \quad (1)$$

where C_i and C_e are the initial and equilibrium concentrations of Pb(II) (mg/L), respectively; V is the volume of Pb(II) solution (L); and w is the weight of EDTA-GO adsorbent (g).

The filtered EDTA-GO adsorbent was then investigated with SEM EDXS to identify the surface element components. The effects of pH on Pb(II) adsorption were measured using the same procedure mentioned above, but the pH values of the solution were adjusted to 2.0, 3.0, 4.5, 5.5, 6.0, 6.8, and 8.2, respectively, with a buffer solution. To test the effect of treatment times on the adsorption process, 20 mg of GO or EDTA-GO was mixed with 100 mL of 100 mg/L Pb(II) solution (6.8). The solution was filtered immediately when the reaction times were reached to 3, 5, 8, 15, 30, 60, 90, and 120 min, respectively. And the Pb(II) concentration remained in filtrate was analyzed for adsorption kinetics analysis.

2.4. Desorption Experiments. To measure the desorption process of Pb(II) on EDTA-GO adsorbents, the preloaded-Pb EDTA-GO adsorbents were prepared using the same procedure mentioned above. The amounts of the loaded Pb(II) on EDTA-Go adsorbent (W_{ad}) were calculated by eq 2.

$$w_{ad} = (c_i - c_e)V \quad (2)$$

where all the parameters are the same as defined before. After being filtered through a 0.2 μm membrane and quickly washed with a buffer solution, the samples were dried in an oven at 100 °C. The Pb-pretreated EDTA-GO was then put in 100 mL of HCl solution with pH adjusted at 2.0, 3.0, 4.0, 5.0, 6.0, and 7.0, respectively. After 4 h of treatment, Pb(II) adsorbed onto EDTA-GO surface was desorbed and dissolved in HCl solution. The solution was then filtered through a 0.2 μm membrane. The filtrate was carefully collected, diluted to 250.0 mL, and used to determine the amount of Pb(II) desorbed from EDTA-GO adsorbent (w_{ds}). After being dried in an oven, the filtered HCl-washed EDTA-GO solid was measured using SEM EDXS. The surface element ratio was calculated from the adsorption strength and the results reflect the surface element enrichment.

The desorption ratio (α_{ds}) was calculated by the equation below

$$\alpha_{ds} = \frac{w_{ds}}{w_{ad}} \quad (3)$$

where w_{ad} is the mass (g) of adsorbed Pb(II) on EDTA-GO adsorbent that was calculated from eq 2, and w_{ds} is the mass (g) of the dissolved Pb(II) from EDTA-GO surface into HCl solution that is calculated from Pb(II) concentration in HCl solution.

As an experimental control, other related carbon materials, such as graphite, activated carbon, GO, RGO, EDTA-RGO, etc., were used to examine the adsorption and desorption behavior using the same procedure mentioned above.

3. RESULTS AND DISCUSSION

3.1. Adsorption Isotherms. Figure 1 shows the adsorption isotherms of Pb (II) at its initial concentration range of 5−300

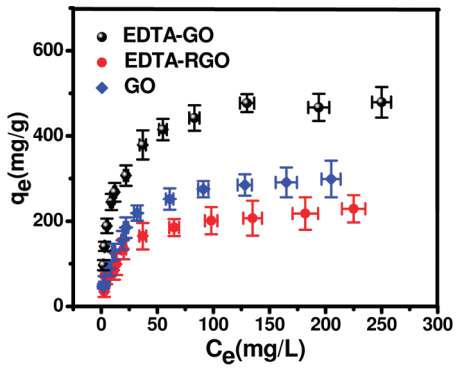

Figure 1. Adsorption isotherms of Pb (II) on three adsorbents at pH 6.8. Experiment conditions: Initial concentration 5−300 mg/L, sample dose 25 mg/200 mL, pH 6.8, temperature (25 ± 2) °C, contact time 24 h.

mg/L (an average of five replicate tests at the same initial concentration). Pb(II) ions are more favorably adsorbed on EDTA-GO and the adsorption capacity of Pb (II) attained ~479 ± 46 mg/g at an equilibrium concentration of 208 ± 17 mg/L, while the adsorption capacity for Pb (II) on GO is 328 ± 39 mg/g. These results are much higher than that obtained from activated carbon and nitric acid treated CNTs.

The experimental data for metal ions adsorption onto GO are analyzed using the Langmuir and Freundlich adsorption isotherm model, which is applicable to highly heterogeneous surfaces. From the linear form of this isotherm, the equation is given as

$$\frac{1}{q_e} = \frac{1}{q_{max}} + \frac{1}{q_{max} K_l C_e} \quad (4)$$

where q_e is the adsorption amount of Pb(II) on adsorbent (mg/g) at an equilibrium state,[15,17,55−57] q_{max} is the adsorption capacity of metals on adsorbent (mg/g), C_e is the equilibrium concentration of metals (mg/g), and K_l is the Langmuir adsorption constant, which is related to the adsorption energy.

For Freundlich model as presented in eq 5

$$q_e = K_f C_e^{1/n} \quad (5)$$

where q_e is the adsorption amount of metals on adsorbent (mg/g), C_e is the equilibrium concentration of metals (mg/g), and K_f and n are Freundlich constants related to adsorption capacity and adsorption intensity, respectively.

It can be seen from the Table 1 that Langmuir model shows a good agreement with the experimental data with a correlation

Table 1. Results and Parameters Associated with Langmuir and Freundlich Models

	Langmuir model			Freundlich model		
materials	q_{max} (mg/g)	K_l (L/mg)	R^2	K_F (mg/g (mg/L)^n)	n	R^2
EDTA-GO	525	0.122	0.975	71.66	2.27	0.933
GO	367	0.035	0.92	10.69	1.29	0.80
EDTA-RGO	228	0.031	0.98	7.38	1.35	0.75

coefficient of 0.975 at pH 6.8. Our investigation demonstrates that Freundlich model fits the results with a correlation coefficient of 0.933. The maximum adsorption capacities of Pb(II) on EDTA-GO and GO from five-times tests are 479 ± 46 and 328 ± 39 mg/g, respectively. These values are greater than that of most carbon-based nanomaterials such as oxidized carbon nanotube and activated carbon.

In addition, EDXS can also be used to track the adsorption process through the analysis of the surface element contents. As shown in Figure 2, the presence of Pb, C, O, Si, and Na at

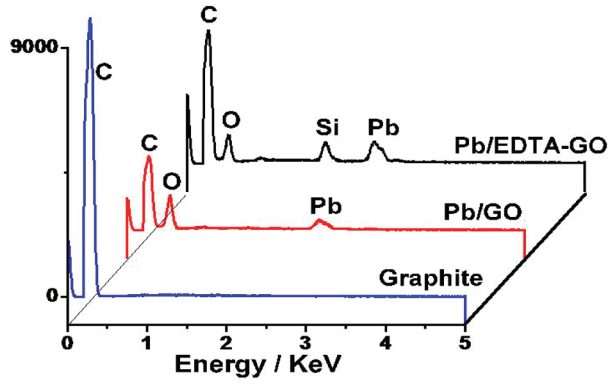

Figure 2. EDXS spectrum of graphite, GO, and EDTA-GO with Pb(II).

EDTA-GO and GO surface is confirmed by the signal of above elements. No signal of Pb element is observed on graphite surface, indicating that no adsorption of Pb occurs at graphite surface. The strong signal of Pb observed at EDTA-GO surface indicates that Pb(II) has been adsorbed onto EDTA-GO surface. Although it is difficult to accurately estimate the surface ratio, the higher EDXS counting ratio of Pb(II) to carbon implies a high adsorption capacity. In addition, the signal strength of Pb at EDTA-GO surface are stronger than that at GO, and the appearance of Si element signal has also confirmed

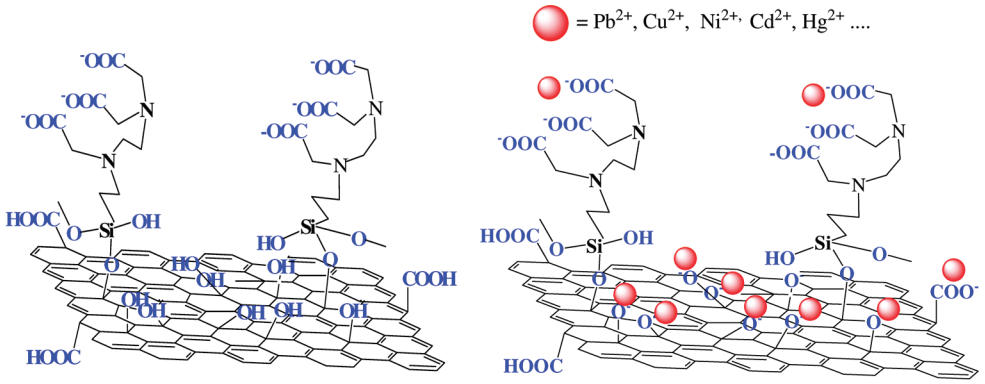

Figure 3. Chemical structure of EDTA-GO (left) and its interaction with heavy metal cations (right).

that presence of EDTA-silane after EDTA groups is introduced on to GO surface, These results suggest that the EDTA group can dramatically increase the adsorption capacities of the heavy metals. In a typical experiment, the surface elements, such as Pb, C, O, and Si, on EDTA-GO are obtained as C+O (72−80%), Pb (26−18%).

3.2. Characterizations of EDTA-GO and Adsorption Mechanism. The adsorption of Pb(II) on a adsorbent can be defined as physical absorption, chemical absorption, and electrostatic attraction. Chemical absorption and electrostatic attraction are two major factors that can affect the adsorption performance of a adsorbent. Generally, a chemical or thermal treatment is necessary to yield higher performance of the traditional carbon-based adsorbents. The chemical and thermal treatment processes can result in great impact on the adsorption capability of activated carbon, carbon fiber and CNTs for metal ions removal because the performance of carbon materials is mainly determined by the nature and concentration of the surface functional groups. For example, the adsorption capacity of the activated carbon and carbon nanotubes increases mainly with the increase of surface density of the surface groups such as carboxylic acids, hydroxyl and carbonyl groups.[13,14,21,22,26,48] Thus, the oxidation of carbon surface can offer not only a more hydrophilic surface structure, but also a larger number of oxygen-containing functional groups, which increases the adsorption capability of carbon material.[24] Thus, it can be predicted that GO can be an ideal adsorbent for heavy metal removal from pollutant and other natural water resources. Figure 3 shows the EDTA-GO and EDTA-GO-metal chemical structures. The synthesis of GO from graphite can introduce a huge amount of −COOH and −OH functional groups onto GO surface, which makes GO become hydrophilic in aqueous solution.[48] When reacted with EDTA-Silane, the hydrolysis of the trialkoxy groups of silane generates -Si−OH groups and the reaction between Si−OH and C−OH of graphene can link EDTA to the graphene surface through Si−O−C bonds. Thus, the chelating groups are introduced onto GO surface.

The above prediction is confirmed by the surface properties of GO and EDTA-GO. The textural characteristics of the as-prepared GO, EDTA-GO are listed in Table 2. The BET surface areas of GO and EDTA-GO powder are determined to be 430 m^2/g and 623 m^2/g, respectively. These results are within the range reported by other authors who found that the BET surface area of the graphene sheets are between 50−1300 m^2/g.[59−63,67] The amount of functional groups formed on the GO and EDTA-GO surface were determined by Boehm's titration method and the results are listed in Table 2. The total amount of acidic group on GO is much higher than that of AC, most of acidified SWCNTs and MWCNTs.[64−66] In addition, after EDTA was linked to GO surface, the amount of basic of EDTA-GO was obtained, which can be attributed to the formation of the amine group on EDTA. Because the adsorption capacity of carbon-based adsorbents mainly depends on the amount of functional groups, the results in Table 2 indicate that the EDTA-GO has the highest adsorption capacity.

Table 2. Amount of Functional Groups on GO, EDTA-GO, EDTA-RGO, and Activated Carbon (AC)

species	S_{Bet} (m^2/g)	total of basicity groups (mmol/g)	total of acidity groups (mmol/g)	capacity for Pb(II) (mg/g)
GO	430	0.2 ± 0.02	6.2 ± 1.3	328 ± 39
EDTA-GO	623	1.8 ± 0.4	8.5 ± 1.9	479 ± 46
EDTA-RGO	730	2.2 ± 0.3	3.0 ± 0.4	204 ± 26
AC	1070[a]	0.27	0.36 ± 0.2	80−120[a]
SWCNTs[a69]	145−1200[a]	n	0.43[a]	30−80[a]
acidified SWCNTs[a70]	77−237[a]	n	1.0−4.5[a]	90[a]
activated carbon cloths[a71]	1689[a]	1.2[a]	1.2[a]	210[a]
activated carbon fiber[a67,72,73]	1375[a]	n	n[a]	40−360[a]

[a]These data are from refs 67−73.

Two adsorption processes are responsible for the removal of Pb(II) with EDTA-GO: ion-exchange reaction between Pb(II) and −COOH or −OH groups and surface complexation and a complex of Pb(II) with EDTA. The first adsorption mechanism is an ion-exchange reaction between Pb(II) and −COOH or −OH groups[71]

(1) Pb(II) reacts with −COOH and −OH groups on GO surface to form a complex

$$GO - COOH + Pb^{2+} \rightarrow GO - COO^{-} - Pb^{2+} + H^{+}$$

$$(GO - COOH)_2 + Pb^{2+} \rightarrow (GO - COO^{-})_2 - Pb^{2+} + 2H^{+}$$

$$GO - OH + Pb^{2+} \rightarrow GO - O^{-} - Pb^{2+} + 2H^{+}$$

$$(GO - OH)_2 + Pb^{2+} \rightarrow (GO - O^-)_2 - Pb^{2+} + 2H^+$$

(2) Pb(II) may also react with COOH groups of EDTA to form a complex with EDTA groups

$$GO - EDTA - COOH + Pb^{2+} \rightarrow GO - EDTA - COO^- - Pb^{2+} + H^+$$

$$(GO - EDTA - COOH)_2 + Pb^{2+} \rightarrow (GO - EDTA - COO^-)_2 - Pb^{2+} + 2H^+$$

The above reaction mechanism is supported by the pH change when the EDTA-GO solution is mixed with a Pb(II) solution. The reaction between −COOH and −OH with Pb(II) releases proton into the solution and then decreases the pH value of the solution.[73] Figure 4 depicts the pH values of solution after

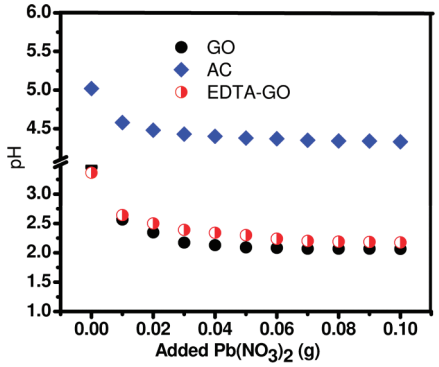

Figure 4. pH change with added $Pb(NO_3)_2$ in 20 mL of DI water with 0.10 g of adsorbent sample.

$Pb(NO_3)_2$ was added to the GO, EDTA-GO and AC solution. In our laboratory experiment, 0.10 g of GO, EDTA-GO or AC sample was added to 20.0 mL DI water, respectively. The initial pH was measured, and GO and EDTA-GO solutions showed lower pH (3.46 and 3.36, respectively). This is because of the dissociation of hydroxyl and carboxyl groups present on GO and EDTA-GO surface. Then, 0.1 mL of 0.10 mg/mL $Pb(NO_3)_2$ solution was injected and pH value was monitored. Upon $Pb(NO_3)_2$ was added to the solution, ion exchange process occurred between −COOH and −OH. Thus, H^+ ion was released from EDTA-GO and GO to the solution, and caused a decrease in pH. The pH decreased when more $Pb(NO_3)_2$ was added to the solution and reached a stable value when all of the surface sites of carboxyl and hydroxyl groups were occupied by Pb(II). For EDTA-GO and GO, the saturated regions were between 0.03−0.06 g $Pb(NO_3)_2$/0.1 g (EDTA-GO or GO). This trend is in agreement with the adsorption capacity. As a controlled experiment, $Pb(NO_3)_2$ added to AC suspension can also cause a decrease of pH, but the amount of $Pb(NO_3)_2$ required to reach a saturated state is less than 0.01 g $Pb(NO_3)_2$ /0.1 g AC. When $Pb(NO_3)_2$ was added to the DI water solutions containing EDTA-GO, GO, and AC, more $[H^+]$ was released from the solutions with EDTA-GO and GO samples than that from the solution with AC sample. This trend is in accordance with the adsorption capacity and also matches AC adsorption capacity for Pb(II) (less than 100 mg/g).

Another mechanism is the formation of complex of EDTA with Pb(II). It is expected that there is a very stable complex formed between EDTA and Pb(II) ions and this will contribute the properties of EDTA-Go to entirely remove Pb(II) from water system.[72] Table 3 lists the removal results after various

Table 3. Removal Efficiency of EDTA-GO Towards Pb(II)

	initial concentration of P(II) (ppb)				
	1.0	5.0	10.0	50.0	100.0
Equilibrium Concentration of P(II) after Being Treated with EDTA-GO (ppb)					
pH 6.5	0.64	0.8	0.73	1.74	5.65
pH 6.8	0.44	0.68	0.87	1.82	5.21
pH 7.2	0.57	0.64	0.73	2.94	4.14

lower concentrations of Pb (II) solutions were treated with EDTA-GO. It can be seen clearly that the Pb(II) concentration in water reached to a safe level after treated with EDTA-GO. The equilibrium concentration of Pb(II) was about 0.5−5 ppb, which is lower than the FDA drinking water standard level (10 ppb). The higher removal efficiency of Pb(II) is probably due to the higher stability constant of Pb(II)-EDTA complex (log $K \approx 18.0$). For a real filtration system, this is an ideal adsorbent because it can remove toxic heavy metals entirely.

3.3. Zeta Potentials of EDTA-GO and the Adsorption Behavior Effect of pH. The adsorption of Pb(II) on the EDTA-GO surface is a surface reaction. It can be predicted that the pH plays an important role in the adsorption of particular metal ions onto GO.[15,58] To evaluate the effect of pH on the adsorption of Pb ions on EDTA-GO, we prepared a series of sample solutions (100.0 mL) containing 100 mg/L Pb(II). The pH values of the solutions were adjusted from 2 to 8.2 with a buffer solution, and 10.0 mg of EDTA-GO was added to above solution separately. After the adsorption was allowed to react for 24 h to achieve the equilibrium state, the solutions were filtered and the Pb(II) concentration in the filtrate (Ce) was analyzed. The adsorption capacity was calculated by eq 1. Figure 5 depicts the relationship between the adsorption

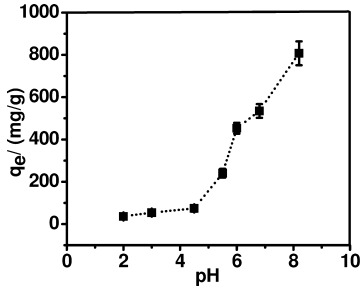

Figure 5. Effect of pH values on the adsorption capacity of Pb(II). Experiment conditions: initial Pb(II) concentration 100 mg/L (100 ppm), sample dose 10 mg/100 mL, temperature (25 ± 2) °C, contact time 24 h.

capacity of Pb(II) on adsorbents and the pH, showing that the adsorption capacity increases with the increasing pH. When pH is less than 5, the adsorption was weak. However, the adsorption of Pb(II) increased with the increasing pH from 5 to 8.2. Generally, the adsorption capacities of metallic species of most adsorbents increase with increases in the pH. In this system, Pb(II) can be adsorbed onto EDTA-GO surface by reacting Pb(II) with EDTA chelating groups, −COOH and −OH groups, respectively. Pb(II) adsorption occurred at lower pH (pH 3) is about 45 mg/g. One explanation could be attributed to the formation of Pb(II)-EDTA chelates on EDTA-

GO surface, such as Pb(II)-HEDTA and Pb(II)-H_2EDTA. Besides this reason, other effects of pH on the adsorbents are surface charge, degree of ionization and speciation. In an acidic solution, the species of surface groups are −COOH and −OH, respectively. The decrease in pH leads to neutralization of surface charge, and thus the adsorption of cations should decrease. In addition, there are some competitions on $-COO^-$ and $-O^-$ sites between proton and metal cations in an acidic condition, which will result in a lower adsorption capacity. The increase in the pH values of the solution will convert more of above groups to $-COO^-$ and $-O^-$, and provide electrostatic interactions that are favorable for adsorbing Pb(II) and other cationic species. These results are also confirmed with zeta potential results of EDTA-GO. Figure 6 depicts that the zeta

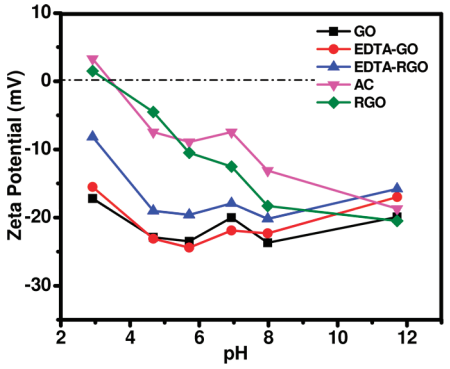

Figure 6. Zeta potentials of carbon materials under various pH conditions.

potential of EDTA-GO decreases first when pH increases from 3 to 6, then exhibits a plateau from 6 to 8 and then increases when pH is 12. The trend of the zeta potential of EDTA-GO is in accordance with the phenomenon observed from oxidized carbon nanotubes.[76,77] It is obvious that in all test pH ranges, EDTA-GO surface is negatively charged, which is due to the functional groups of EDTA-GO that can be ionized to make EDTA-GO be negative in solutions and can provide stronger electrostatic interactions between metal cations and the adsorbents. At the same pH, the zeta potential of EDTA-GO and GO were more negative than that of AC, EDTA-RGO, and RGO, which indicates that the amounts of −COOH and −OH of EDTA-GO and GO is the highest among the above adsorbents. These results are in consistent with the absorption capacity and the surface acidity groups presented in Table 2.

However, it should be pointed out that a high pH value, for example, pH value >8.0, will cause a hydrolysis process of metal cations and form metal hydroxide, such as $Pb(OH)^+$, $Pb(OH)_2$, etc.[74−77] In this condition, the removed Pb(II) will be divided into two clusters: the adsorption and the precipitation of lead hydroxide. The test of the precipitation of Pb at different pH values was obtained by mixing 1.0 mL 100 mg/L standard Pb (II) solution with a series of pH buffer solutions (10.0 mL). The pH values are 5.5, 6.5, 6.8, 7.0, 7.2, 7.5, 8.2, and 9.5, respectively. The mixture solutions were left overnight and the Pb(II) precipitation was formed on the bottom of the beakers and then the upper clear solutions were used for analyzing the remained Pb(II) concentration with AAS. It was found that when pH is higher than 7.2, a precipitation of Pb(II) occurs, when pH is lower than 7.0, no precipitation was found. Therefore, the optimized adsorption pH value was performed at pH 6.5−7.0. Under these conditions, no precipitation of Pb(II) occurred and then all of the removed Pb(II) from the solution were adsorbed on EDTA-Go surface. Therefore, our experiment was performed at pH 6.8 in order to avoid any precipitation at higher pH values except when high pH was needed for investigation purpose. At pH 6.8 in NH_3−NH_4Cl buffer, no precipitation of lead was observed and 100% of Pb species was water-soluble. Pb(II) was removed by adsorption only.

3.4. Effect of Treatment Times. The adsorption behavior of Pb(II) by GO and EDTA-GO in relation to contact time was carried out by varying the treatment times from 5 min to 2 h for a 100 mL of 100 mg/L Pb(II) solution with a dose of adsorbent of 20 mg at an optimum pH of 6.8. The adsorption process was investigated with and without the sonication treatment. The adsorption equilibrium capacity was obtained by mixed the adsorbents with Pb(II) solution for 24 h, which are believed to be equilibrium state. The percent (%) of adsorption equilibrium capacity was calculated by divided the adsorbed amounts of Pb(II) on adsorbents at different times by the adsorption equilibrium capacity. The results are presented in Figure 7. It was found that, without a sonication treatment, the

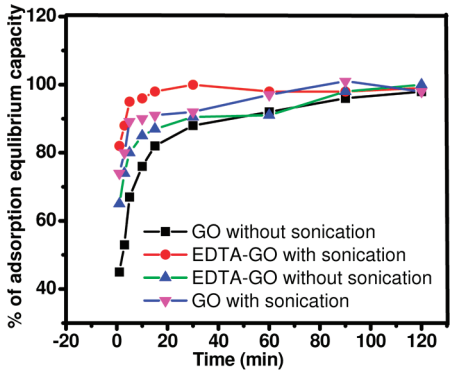

Figure 7. Effect of contact time on the adsorption capacity of Pb(II). Experiment conditions: initial Pb(II) concentration 100 mg/L (100 ppm), sample dose 20 mg/100 mL, temperature (25 ± 2) °C.

time for the adsorption to reach the equilibrium state for EDTA-GO and GO were 20−30 min and 30−45 min, respectively, with the ratio to reach the maximum adsorption capacities of 90−95%. With a sonication treatment, the adsorption reached to the equilibrium state within 5−15 min for the EDTA-GO and GO with 90−95% of the maximum adsorption capacities. As a comparison, it took some commercial adsorbents about 1 to 24 h.[40] This rapid adsorption was directly owed to the 2D structure of EDTA-GO because this 2D structure enables the adsorbents to be ready for accessibility of the chelating EDTA, making it easy for metal chelation. This short equilibrium time indicates that GO has a strong potential application for metal ion adsorption.

The effect of the initial concentration of Pb (II) on the adsorption rate was also investigated. It was found that the adsorption capacity of Pb(II) onto EDTA-GO reached 90% of its equilibrium state in about 11, 15, and 18 min when the initial concentrations (C_i) of Pb(II) were 10, 50, and 100 mg/L, respectively. It is apparent that the adsorption rate achieved to equilibrium state is faster at a lower initial heavy metal concentration (C_i), probably because the adsorption site adsorbed the available metal ions more rapidly at a lower C_i. This rate is much faster than other carbon based adsorbents, such as AC, carbon nanotubes and other materials.[17,45,55] The

time required to reach the equilibrium state is much shorter than AC and other carbon based adsorbents, indicating a commercially available product of GO for the waste treatment.

3.5. Desorption Process. The adsorption capacity and the desorption property are two key parameters to evaluate a adsorbent. An ideal adsorbent should not only possess higher adsorption capability, but also show better desorption property, which will significantly reduce the overall cost for the adsorbents. Figure 8 gives the desorption ratio of EDTA-GO

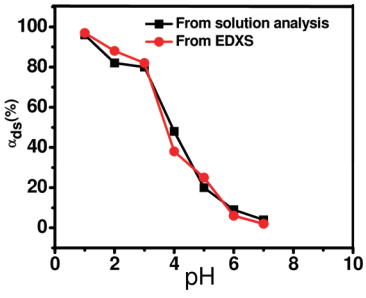

Figure 8. Desorption Ratio (α_{ds}) of EDTA-GO toward Pb(II) at Different pH HC Solution.

with Pb(II). It is apparent that Pb(II) desorption increased with decreasing pH values. Only about 9−15% of Pb(II) adsorbed onto GO surface was desorbed from EDTA-GO surface using washing solution at pH >6, then increased sharply at pH <5.0, and eventually reached about 90% at pH <2.0.

To further investigate the desorption process, we applied EDXS technique to monitor the surface element components of the EDTA-GO and GO sample before and after the washing process. The strength of Pb signal at EDTA-GO surface was used to estimate the desorption process. Figure 9 depicts a

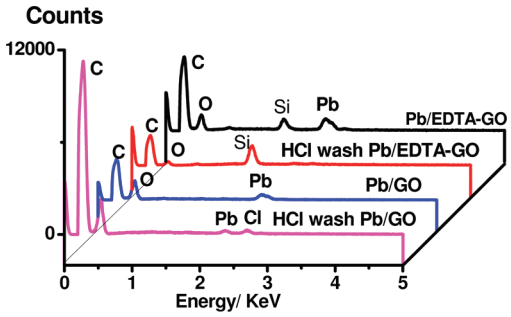

Figure 9. EDXS data of preloaded Pb(II) sample before and after washing with 0.10 M HCl.

series of EDXS spectrum of Pb-pretreated GO, and EDTA-GO samples before and after the HCl washing process. After the washing process, the signal of Pb was diminished, which confirms the complete desorption process. Pb(II) absorbed on EDTA-surface was washed out through the process. In a typical sample, the surface element ratio (mass) of Pb on EDTA-GO surface decreased from 15.8 to 1.2%, implying that almost all the Pb (92%) can be removed by HCl within 1 h. This result is in a good agreement with the AAS result (Figure 8), proving that Pb(II) adsorbed by EDTA-GO can be easily desorbed and, therefore, EDTA-GO can be employed repeatedly for heavy metal removal. Further research demonstrates that the capacity of EDTA-GO for Pb(II) removal was maintained at 80% of its initial capacity after about 10 cycles. These data confirm that GO is an ideal heavy metal adsorbent.

4. CONCLUSIONS

The introduction of EDTA groups to the GO surface through silanization process can significantly increase the adsorption capacity of GO for heavy metal removal. The EDTA groups together with −OH and −COOH groups on the GO surface can make EDTA-GO an excellent adsorbent for removal of toxic heavy metals, such as Pb(II), Cu(II), Ni(II) and Cd(II) in aqueous solution. The adsorption of Pb(II) fits the Langmuir equation well. The highest adsorption capacity varies with pH of the solution. The highest adsorption capacity of EDTA-GO for Pb(II) is found to be 479 ± 46 mg/g, which is 4−5 times higher than that of oxidized carbon nanotubes, and 1−2 times higher than that of GO. It was found in this study that the Pb(II) adsorption processes reached their equilibrium state within 10 to 30 min, which is faster than most of carbon-based adsorbents can do. On the other hand, the desorption behavior of metals on the GO surface suggests that GO can be reused after treated with HCl solution. This research demonstrates that EDTA-GO can be an effective adsorbent for toxic heavy metal removal.

AUTHOR INFORMATION

Corresponding Author

*Tel: +1 973-655-7118. E-mail: hous@mail.montclair.edu.

Notes

The authors declare no competing financial interest.

ACKNOWLEDGMENTS

The authors are grateful for the financial support from Montclair State University Startup Funding, Margaret and Herman Sokol Foundation, Sokol Institute Student-Faculty Research Grants, and the National Natural Science Foundation of China (21175059).

REFERENCES

(1) Juwarkar, A. A.; Singh, S. K.; Mudhoo, A. *Rev. Environ. Sci. Biol.* **2010**, *9*, 215.
(2) Nagajyoti, P. C.; Lee, K. D.; Sreekanth, T. V. M *Environ. Chem. Lett.* **2010**, *8*, 199.
(3) Fu, F. L.; Wang, Q. *J. Environ. Manage.* **2011**, *92*, 407.
(4) Rao, M. M.; Ramana, D. K.; Seshaiah, K.; Wang, M. C.; Chien, S. W. C. *J. Hazard. Mater.* **2009**, *166*, 1006.
(5) Solanki, P.; Gupta, V.; Kulshrestha, R. *E-J. Chem.* **2010**, *7*, 1200.
(6) Cai, G. B.; Zhao, G. X.; Wang, X. K.; Yu, S. H. *J. Phys. Chem. C* **2010**, *114*, 12948.
(7) Fu, F.; Zeng, H.; Cai, Q.; Qiu, R.; Yu, J.; Xiong, Y. *Chemosphere* **2007**, *69*, 1783.
(8) Mauter, M. S.; Elimelech, M. *Environ. Sci. Technol.* **2008**, *42*, 5843.
(9) Macaskie, L. E.; Mikheenko, I. P.; Yong, P.; Deplanche, K.; Murray, A. J.; Paterson-Beedle, M.; Coker, V. S.; Pearce, C. I.; Cutting, R.; Pattrick, R. A. D.; Vaughan, D.; van der Laan, G.; Lloyd, J. R. *Hydrometallurgy* **2010**, *104*, 483.
(10) Pradeep, T.; Anshup. *Thin Solid Films* **2009**, *517*, 6441.
(11) Ruparelia, J. P.; Duttagupta, S. P.; Chatterjee, A. K.; Mukherji, S. *Desalination* **2008**, *232*, 145.
(12) Petosa, A. R.; Jaisi, D. P.; Quevedo, I. R.; Elimelech, M.; Tufenkji, N. *Environ. Sci. Technol.* **2010**, *44*, 6532.
(13) Rao, G. P.; Lu, C.; Su, F. *Sep. Purif. Technol.* **2007**, *58*, 224.
(14) Stafiej, A.; Pyrzynska, K. *Sep. Purif. Technol.* **2007**, *58*, 49.

(15) Tawabini, B.; Al-Khaldi, S.; Atieh, M.; Khaled, M. *Water Sci. Technol.* **2010**, *61*, 591.
(16) Pyrzynska, K.; Bystrzejewski, M. *Colloids Surf., A* **2010**, *362*, 102.
(17) Pyrzynska, K. *Microchim. Acta* **2010**, *169*, 7.
(18) Kadirvelu, K.; Faur-Brasquet, C.; Le Cloirec, P. *Langmuir* **2000**, *16*, 8404.
(19) Goel, J.; Kadirvelu, K.; Rajagopal, C.; Garg, V. K. *Ind. Eng. Chem. Res.* **2005**, *44*, 1987.
(20) Atieh, M. A.; Bakather, O. Y.; Al-Tawbini, B.; Bukhari, A. A.; Abuilaiwi, F. A.; Fettouhi, M. B. *Bioinorg. Chem. Appl.* **2010**, 1.
(21) Xu, Y. J.; Arrigo, R.; Liu, X.; Su, D. S. *New Carbon Mater.* **2011**, *26*, 57.
(22) Wang, H. J.; Zhou, A. L.; Peng, F.; Yu, H.; Chen, L. F. *Mater. Sci. Eng., A* **2007**, *466*, 201.
(23) Chen, C. L.; Wang, X. K. *Ind. Eng. Chem. Res.* **2006**, *45*, 9144.
(24) Schierz, A.; Zanker, H. *Environ. Pollut.* **2009**, *157*, 1088.
(25) Ion, A. C.; Ion, I.; Culetu, A. *Mater. Sci. Eng., B* **2011**, *176*, 504.
(26) Wang, H. J.; Zhou, A. L.; Peng, F.; Yu, H.; Yang, J. *J. Colloid Interface Sci.* **2007**, *316*, 277.
(27) Ruoff, R. *Nat. Nanotechnol.* **2008**, *3*, 10.
(28) Park, S.; Ruoff, R. S. *Nat. Nanotechnol.* **2009**, *4*, 217.
(29) Moon, I. K.; Lee, J.; Ruoff, R. S.; Lee, H. *Nat. Commun.* **2010**, 1.
(30) Park, S.; An, J. H.; Jung, I. W.; Piner, R. D.; An, S. J.; Li, X. S.; Velamakanni, A.; Ruoff, R. S. *Nano Lett* **2009**, *9*, 1593.
(31) Dreyer, D. R.; Park, S.; Bielawski, C. W.; Ruoff, R. S. *Chem. Soc. Rev.* **2010**, *39*, 228.
(32) Sreeprasad, T. S.; Maliyekkal, S. M.; Lisha, K. P.; Pradeep, T. *J. Hazard. Mater.* **2011**, *186*, 921.
(33) Zhang, T.; Cheng, Z. G.; Wang, Y. B.; Li, Z. J.; Wang, C. X.; Li, Y. B.; Fang, Y. *Nano Lett.* **2010**, *10*, 4738.
(34) Li, J.; Guo, S. J.; Zhai, Y. M.; Wang, E. K. *Anal. Chim. Acta* **2009**, *649*, 196.
(35) Deng, X. J.; Lu, L. L.; Li, H. W.; Luo, F. *J. Hazard. Mater.* **2010**, *183*, 923.
(36) Yang, S. T.; Chang, Y. L.; Wang, H. F.; Liu, G. B.; Chen, S.; Wang, Y. W.; Liu, Y. F.; Cao, A. N. *J. Colloid Interface Sci.* **2010**, *351*, 122.
(37) Petit, C.; Mendoza, B.; Bandosz, T. J. *Chemphyschem* **2010**, *11*, 3678.
(38) Petit, C.; Mendoza, B.; Bandosz, T. J. *Langmuir* **2010**, *26*, 15302.
(39) Lee, J. H.; Kim, B. S.; Lee, J. C.; Park, S. *Eco-Materials Processing & Design VI*; Trans Tech Publications: Zurich, Switzerland, 2005; Vol. *486−487*, p 510
(40) Repo, E.; Warchol, J. K.; Bhatnagar, A.; Sillanpaa, M. J *Colloid Interface Sci.* **2011**, *358*, 261.
(41) Repo, E.; Malinen, L.; Koivula, R.; Harjula, R.; Sillanpaa, M. *J. Hazard. Mater.* **2011**, *187*, 122.
(42) Yang, L. Q.; Li, Y. F.; Wang, L. Y.; Zhang, Y.; Ma, X. J.; Ye, Z. F. *J. Hazard. Mater.* **2010**, *180*, 98.
(43) Zhang, Y.; Li, Y. F.; Yang, L. Q.; Ma, X. J.; Wang, L. Y.; Ye, Z. F. *J. Hazard. Mater.* **2010**, *178*, 1046.
(44) Tejowulan, R. S.; Hendershot, W. H. *Environ. Pollut.* **1998**, *103*, 135.
(45) Repo, E.; Warchol, J. K.; Kurniawan, T. A.; Sillanpaa, M. E. T. *Chem. Eng. J.* **2010**, *161*, 73.
(46) Nabi, S. A.; Naushad, M.; Bushra, R. *Adsorpt. Sci. Technol.* **2009**, *27*, 423.
(47) Hou, S. F.; Kasner, M. L.; Su, S. J.; Patel, K.; Cuellari, R. *J. Phys. Chem. C* **2010**, *114*, 14915.
(48) Hou, S. F.; Su, S. J.; Kasner, M. L.; Shah, P.; Patel, K.; Madarang, C. J. *Chem. Phys. Lett.* **2010**, *501*, 68.
(49) Wietecha, M. S.; Zhu, J.; Gao, G.; Wang, N.; Feng, H.; Gorring, M. L.; Kasner, M. L.; Hou, S. *J. Power Source* **2012**, *198*, 30.
(50) Hummers, W. S.; Offeman, R. E. *J. Am. Chem. Soc.* **1958**, *80*, 1339.
(51) Fletcher, A. J.; Uygur, Y.; Thomas, K. M. *J. Phys. Chem. C* **2007**, *111*, 8349.
(52) Marshall, M. W.; Popa-Nita, S.; Shapter, J. G. *Carbon* **2006**, *44*, 1137.
(53) Lopez-Ramon, M. V.; Stoeckli, F.; Moreno-Castilla, C.; Carrasco-Marin, F. *Carbon* **1999**, *37*, 1215.
(54) Shen, W.; Li, Z.; Liu, Y. *Rec. Pat. Chem. Eng.* **2008**, *1*, 27.
(55) Moradi, O.; Zare, K.; Monajjemi, M.; Yari, M.; Aghaie, H. *Fullerenes, Nanotubes, Carbon Nanostruct.* **2010**, *18*, 285.
(56)
(57) Vukovic, G. D.; Marinkovic, A. D.; Colic, M.; Ristic, M. D.; Aleksic, R.; Peric-Grujic, A. A.; Uskokovic, P. S. *Chem. Eng. J.* **2010**, *157*, 238.
(58) Atieh, M. A.; Bakather, O. Y.; Tawabini, B. S.; Bukhari, A. A.; Khaled, M.; Alharthi, M.; Fettouhi, M.; Abuilaiwi, F. A. *J. Nanomater.* **2010**, *2010*, 1.
(59) Chandra, V.; Park, J.; Chun, Y.; Lee, J. W.; Hwang, I.-C.; Kim, K. S. *ACS Nano* **2010**, *4*, 3979.
(60) Zhu, Y.; Murali, S.; Ca, W.; Li, X.; Suk, J. W.; Potts, J. R.; Ruoff, R. S. *Adv. Mater.* **2010**, *22*, 3906.
(61) Park, S.; An, A.; Potts, J. R.; Velamakanni, A.; Murali, H.; Ruoff, R. S. *Carbon* **2011**, *49*, 3019.
(62) Sasha Stankovich, S.; Dikin, D. A.; Piner, R. D.; Kohlhaas, K. A.; Kleinhammes, A.; Jia, Y.; Wu, Y.; Nguyen, S. T.; Ruoff, R. S. *Carbon* **2007**, *45*, 1558.
(63) Yang, S.; Feng, X.; Wang, L.; Tang, K.; Maier, J.; Müllen, K. *Angew. Chem., Int. Ed.* **2010**, *49*, 4795.
(64) Scheibe, B.; Borowiak-Palen, E.; Kalenczuk, R. J. *Mater. Character.* **2010**, *61*, 185.
(65) Kandah, M. I.; Meunier, J.-L. *J. Hazard. Mater.* **2007**, *146*, 283.
(66) Li, Y.-H.; Wang, S.; Luan, Z.; Ding, J.; Xu, C.; Wu, D. *Carbon* **2003**, *41*, 1057.
(67) Chakraborty, A.; Deva, D.; Sharma, A.; Verma, A. *J. Colloid Interface Sci.* **2011**, *359*, 228.
(68) Li, Y. H.; Di, Z. C.; Ding, J.; Wu, D. H.; Luan, Z. K.; Zhu, Y. Q. *Water Res.* **2005**, *39*, 605.
(69) Wang, H. J.; Zhou, A. L.; Peng, F.; Yu, H.; Chen, L. F. *Mater. Sci. Eng.* **2007**, *466*, 201.
(70) Ga, Z.; Bandosz, T. J.; Zhao, Z'; Han, M.; Qiu, J. *J. Hazard. Mater.* **2009**, *167*, 357.
(71) Ladirvelu, K.; Faur-Brasquet, C.; Le Cloirec, P. *Langmuir* **2000**, *16*, 8404.
(72) Leyva-Ramos, R.; Berber-Mendoza, M. S.; Salazar-Rabago, J.; Guerrero-Coronado, R. M.; Mendoza-Barron, J. *Adsorption* **2011**, *17*, 515.
(73) Harry, I. D.; Saha, B.; Cumming, I. W. *J. Colloid Interface Sci.* **2006**, *304*, 9.
(74) Xu, D.; Tan, X.; Chen, C.; Wang, X. *J. Hazard. Mater.* **2008**, *154*, 407.
(75) Machida, M.; Mochimaru, T.; Tatsumoto, H. *Carbon* **2006**, *44*, 2681.
(76) Wang, J. J.; Zgou, A. J.; Peng, F.; Yu, H.; Chen, L. F. *Mater. Sci. Eng* **2007**, *466*, 201.
(77) Lu, C.; Chiu, H. *Chem. Eng. J.* **2008**, *139*, 462.